



25th ABCM International Congress of Mechanical Engineering
October 20-25, 2019, Uberlândia, MG, Brazil

COBEM-2019-1939

Numerical Study of the Velocity Field for a Jet in a Crossflow using Linear and Non-Linear Turbulence Models

Kelvin Cristófal de Moraes

Embraer S. A., Avenida Brigadeiro Faria Lima, 2170, São José dos Campos - SP, Brazil. 12227-901
Instituto Tecnológico de Aeronáutica, Praça Marechal Eduardo Gomes, 50, São José dos Campos - SP, Brazil. 12228-900
kelvin.morais@embraer.com.br

Claudia Regina de Andrade

Instituto Tecnológico de Aeronáutica, Praça Marechal Eduardo Gomes, 50, São José dos Campos - SP, Brazil. 12228-900
claudia@ita.br

Luis Carlos de Castro Santos

Embraer S. A., Avenida Brigadeiro Faria Lima, 2170, São José dos Campos - SP, Brazil. 12227-901
Universidade de São Paulo, Rua do Matão, 1010, São Paulo-SP, Brazil. 05508-900
luis.castro@embraer.com.br

Abstract. A numerical study of a jet in a cross stream has been carried to investigate the accuracy of standard linear and non-linear turbulence models in predicting the flow field for a jet in cross flow. A mesh dependence study was performed for hexahedral and hybrid meshes in 3 levels of global refinement and an important influence of the velocity ratio and mesh topology was found in the grid convergence behavior. An earlier work with a heated jet in cross flow showed a great improvement in the numerical temperature field using a non-linear turbulence model. In this work, the same turbulence models were tested for an unheated jet and the velocity profiles were compared to experimental data. However, only a slight improvement was noticed using the non-linear turbulence model. Current RANS models fail in predicting the development of the jet in the cross stream.

Keywords: CFD, Turbulence Modeling, RANS, Jets in Crossflow

1. INTRODUCTION

Jets discharging in a cross flow is a configuration present in a wide range of applications. This type of flow is established every time a jet is exhausted in a cross stream. In aerospace industry, for example, two very representative examples are the cooling of turbine blades and the discharge flow produced by auxiliary system air outlets. In the first case, a series of cooled jets are discharged by means of internal channels inside the blade, creating a cooled film that protects the blade surface materials from high temperatures inside the aircraft engine. In the second application, a heated air jet from internal systems are exhausted in the external flow outside the airplane. The interaction of the heated jet with the external flow deflects the jet into the aircraft surface, locally rising the temperature and forcing the use of materials resistant to high temperatures near the outlet that are generally more expensive and heavy.

The flow dynamics for jets in cross flow is the topic of several experimental studies since the second part of the last century. Most part of them were focused in characterizing the main flow features through measurements of the velocity and temperature distribution downstream the jet outlet as well as flow visualization to improve the understanding of mixture process between the jet and the cross stream. Up to now, it is known that the flow dynamics of a jet in a cross flow is the result of the interaction between several canonical flows. First, there is round jet penetrating the boundary layer of a cross stream. This jet is deflected in the main stream direction and gives rise to a counter rotating vortex pair, the first coherent structure seen in this type of flow. The penetration of jet is associated with the *momentum* or *velocity ratio* (Kamotani and Greber, 1972), a parameter that stands for the relative strength of the jet in comparison to the external flow. The velocity ratio, V_R , is defined as the ratio of the internal flow velocity, V_J , and the cross stream velocity, V_∞ . Thus, as the jet becomes stronger, it penetrates more in the cross stream and its effects are observed for larger distances in the flow direction (Bergeles *et al.*, 1976). For the cross stream, the jet is seen as an obstacle, giving rise to a horseshoe upstream the jet outlet and a wake downstream the jet (Kelso *et al.*, 1996). Depending on the jet Reynolds number, hovering vortex can also appear as a result of instabilities in the round jet shear layer (Fric and Roshko, 1991). A scheme of the flow field for a jet in cross flow with the coherent structures proposed by Kelso *et al.* (1996) is presented on figure 1.

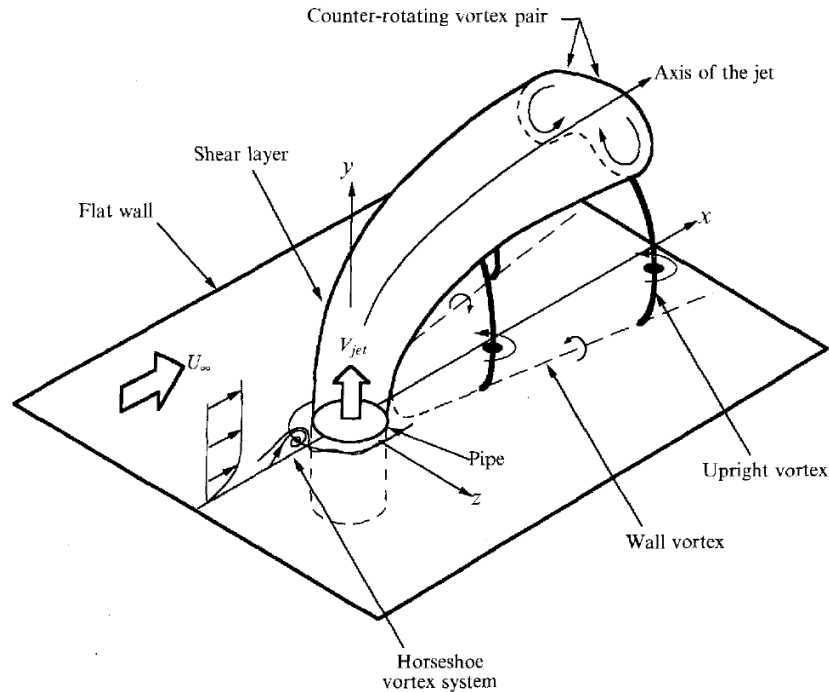


Figure 1. A scheme of the coherent structures developed behind a jet in a cross stream. This figure has been extract from the work of Kelso *et al.* (1996)

The high complex flow dynamics presented above is one of the main challenges for accurate numerical predictions of the flow field for such flows. RANS based numerical studies for jets in cross flow shows that standard turbulence models fail in predicting accurately the entire flow field. Generally, they present lower spreading rates in comparison to experimental results, producing a more dense jet core. Recent studies with Hybrid RANS-LES techniques as well as pure LES simulations showed extraordinary improvement in the numerical results (Prause *et al.*, 2016). However, those techniques are far from being the main numerical method used in industry due to high computational effort needed for those simulations. Thus, it is almost required the development and tests of more elaborated turbulence models that can handle with complex flows like jets in cross flow.

This work is the second step of a numerical study intending to determine the accuracy of RANS methods in predicting the flow field of heated jets in a crossflow. In the first step of the study (Morais *et al.*, 2018), the experiment of Ramsey and Goldstein (1971) for a heated jet issuing perpendicularly in a cross stream was reproduced numerically using linear and non-linear turbulence models. Numerical temperature profiles for each turbulence model were compared with experimental data, showing that standard turbulence models present a lower spreading rate in comparison to experiment. An interesting improvement was observed using a non-linear turbulence model, namely *Hellsten* (Hellsten, 2005). This turbulence model was developed for high-lift configurations where severe adverse pressure gradients are present and flow separation might occur along the airfoil. This feature is also presented behind the jet wake for the current application and it is possible that the improvement seen in the computed temperature field is due to a better representation of the jet wake, enhancing the entire prediction of the flow field. However, only the temperature field was properly compared in this work, due to lack of detailed velocity measurements. In this work, a new experiment is assessed with the same turbulence models used in the last work to verify if the non-linear *Hellsten* model is in fact better solving the entrainment of the jet flow with the cross stream or the improvement seen in the temperature field is just a matter of increased diffusivity.

2. METHODOLOGY

In this work the accuracy in predicting the velocity field for a jet in a cross flow using linear and non-linear turbulence models will be assessed through the numerical reproduction of the experiment of Andreopoulos and Rodi (1984) briefly described in the next subsection. The study was divided in three steps. The first step is a mesh dependence study where the effects of grid refinement and topology along the flow domain will be discussed for one turbulence model. In this step, one mesh will be defined to perform the next studies based on the mesh size and accuracy. In the next steps, the velocity profiles predicted by linear and non-linear turbulence models will be investigated in the duct near the exit plane (second step) as well as its interactions with the external outside the duct (third step).

2.1 Experimental Data

The source of experimental data for the velocity field is the experiment conducted by Andreopoulos and Rodi (1984) for a circular jet in a crossflow. In this work, a flat plate was placed inside the test section of a subsonic wind tunnel and the jet was created through a compressor that fed air into a plenum chamber attached to a straight pipe of 50mm internal diameter and $12D$ long. Both streams were tripped to assess a fully turbulent flow. The cross stream velocity was 13.9m/s with a turbulence level of 0.05 percent. Also, a boundary layer thickness of $0.278D$ and a friction coefficient of $C_f = 0.0037$ was measured $4D$ upstream the exit hole where the effects of jet in the cross stream are negligible. The experiment was conducted with a constant external stream for blowing ratios of 0.5, 1.0 and 2.0. It means that the jet mass flow rate was adjusted in order to assess the desired velocity ratio. The jet Reynolds number for the velocity ratios above are 20500, 41000 and 82000. Measurements of velocity profiles and turbulent quantities were done downstream the jet exit plane, providing an excellent characterization of the flow field in the jet lee.

2.2 Numerical method

The commercial software CFD++ (Peroomian *et al.*, 1997), from Metacomp Technologies, has been used in the present work as the CFD solver. All further simulations were conducted in a steady state approach using a preconditioned density-based solver for the RANS equations. A second-order spatial discretization scheme and an implicit time integration scheme has been used. Linear and non-linear turbulence models were tested in order to assess possible differences in the computation of numerical velocity field. The linear turbulence models chosen for this work are highly used in aerospace industry, namely the realizable $k - \varepsilon$ (Shih *et al.*, 1995) and SST (Menter, 1994). The non-linear turbulence model is a model developed originally for high lift configurations called *Hellsten*. The convergence of numerical simulations are evaluated in terms of the mass flow rate in the outlet boundary condition, the drop of relative residuals as well as the forces in every boundary condition.

2.3 Computational Domain and Boundary Conditions

The computational domain consists of a circular cross section duct mounted flush in a flat plate. The duct was positioned $10D$ downstream the flat plate leading edge, following the experimental work setup in order to reproduce the same boundary layer flow. The flat plate bounds were dimensioned long enough to avoid effects of wall proximity and flow blockage; its dimensions are presented on figure 2. The duct is $12D$ long and it is connected to a plenum chamber by means of a contraction zone to account for any flow feature induced at the contraction zone and increase geometrical fidelity.

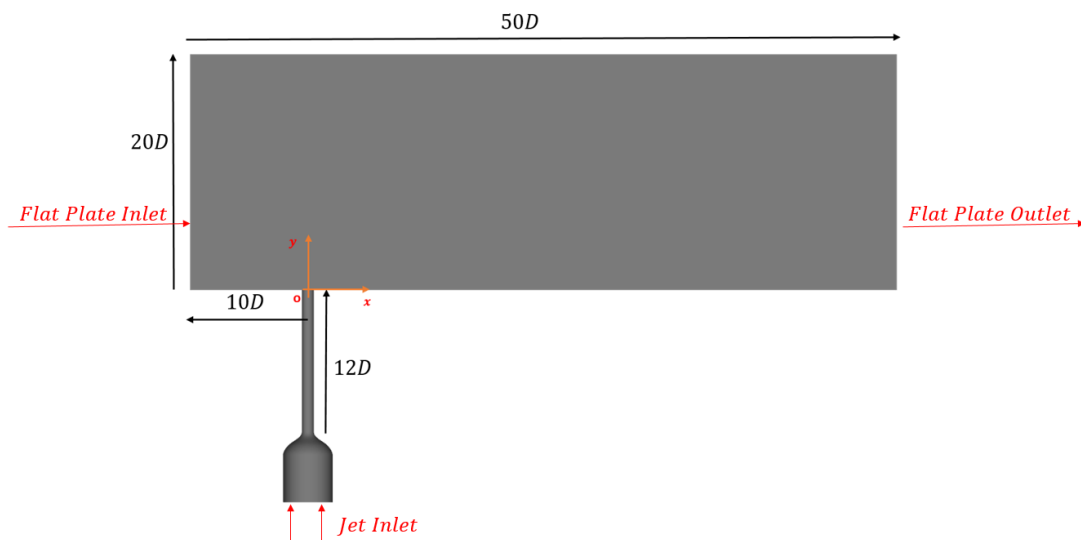


Figure 2. Computational domain and inflow boundary conditions

The flat plate flow was modelled through a velocity inlet boundary condition at the flat plate entrance and a back pressure imposition at the outlet. A mass flow boundary condition was placed in the jet inlet, varying total pressure with a mass flow rate target. The duct and flat plate boundaries were modelled as no slip walls using a solve to the wall formulation. As the problem presents symmetry in the span wise direction, a symmetry boundary condition was placed in the jet centerline plane. Simulations were done for $V_R = 0.5, 1.0$ and 2.0 with the external velocity fixed at $V_\infty = 13.9\text{m/s}$.

2.4 Computational Mesh

In order to perform a grid dependence study, six grids have been developed to support the discussions about the effect of mesh refinement and topology in the numerical results. The meshes are divided in hexahedral and hybrid meshes and subdivided in three refinement levels: Coarse, Medium and Fine. The purpose of using two mesh topologies relies on the fact that hexahedral meshes represent a standard approach for academic refinement while the hybrid meshes represent the industrial practice. In real applications, sometimes it is impossible to produce a pure blocked hexahedral mesh and one has to use the hybrid approach. Thus it is important to investigate the mesh refinement effects on both mesh strategies.

The meshes were globally refined, increasing the number of elements in each spatial dimensional by a factor of 2. It means the number of cells increase in a factor 2^3 for every level of mesh refinement, as the geometry is tridimensional. Table 1 presents a summary of mesh types and sizes.

Table 1. Summary of grids used in the mesh dependence study

Mesh Description	Mesh Topology	Number of Cells
Hyb-Coarse	Hybrid	0.6M
Hyb-Medium	Hybrid	5.2M
Hyb-Fine	Hybrid	33.7M
Hex-Coarse	Hexahedral	0.4M
Hex-Medium	Hexahedral	3.7M
Hex-Fine	Hexahedral	24.9M

Every mesh were generated keeping the first cell height constant, ensuring that $Y^+ < 1$ in the walls for all velocity ratios analyzed. Moreover, all grids have been created with a local refinement region near the jet outlet to increase mesh resolution where severe flow gradients are expected.

The hybrid meshes are composed of prismatic elements near the wall and tetrahedral elements to fulfill the surrounding volume outside the near wall regions. Two density zones were created. The first density zone is responsible for a higher mesh refinement near the jet exit and a second zone was created surrounding the jet trajectory to keep the volumes under a certain limit. The hexahedral is a multiblock structured mesh with an increase mesh resolution near the exit hole. Figure 3 presents the numerical mesh at the symmetry plane where the refinement levels can be visualized.

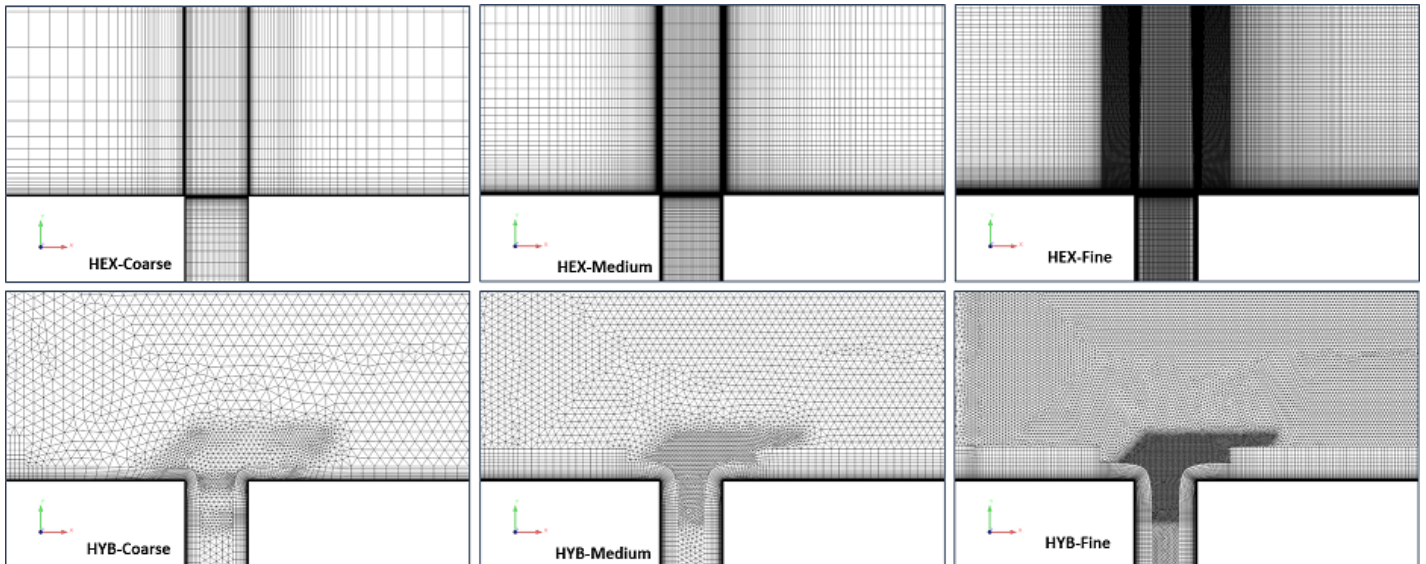


Figure 3. Computational grid at the flat plate symmetry plane for hybrid and hexahedral meshes for 3 levels of mesh refinement

3. Results and Discussion

Numerical results assessed with different grid refinements (Coarse, Medium and Fine) and topologies (Hybrid and Hexahedral) are presented on figure 4, 5 and 6 for velocity ratios ranging from 0.5 to 2.0. The results are presented as velocity profiles in several longitudinal position along the flat plate. It is important to keep in mind that these simulations were run with the realizable $k - \varepsilon$ turbulence model only.

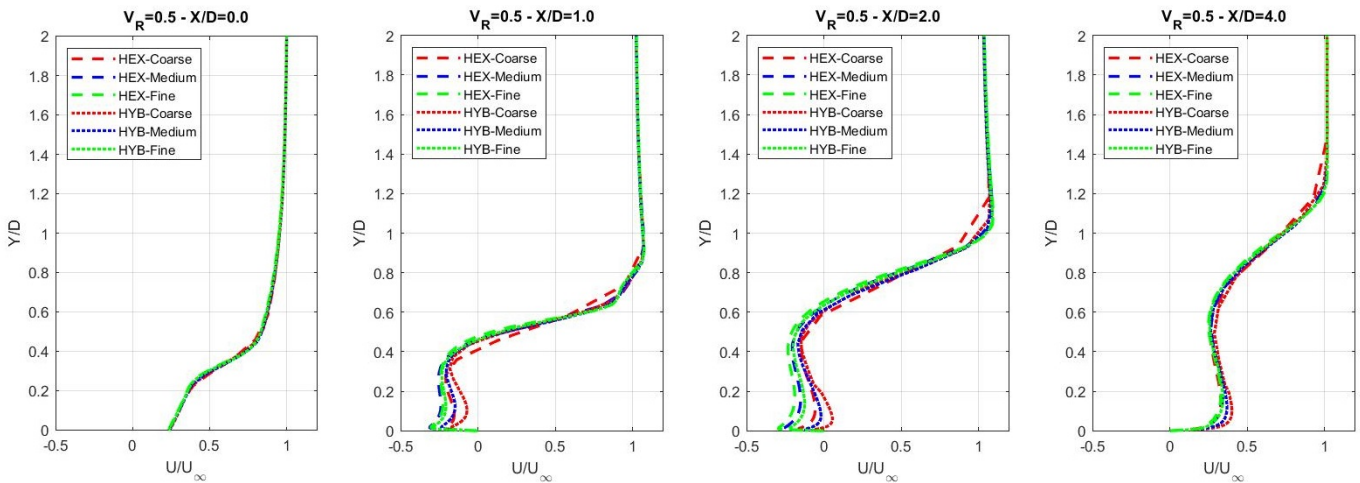


Figure 4. Grid Refinement effects on the numerical solution for $V_R = 0.5$

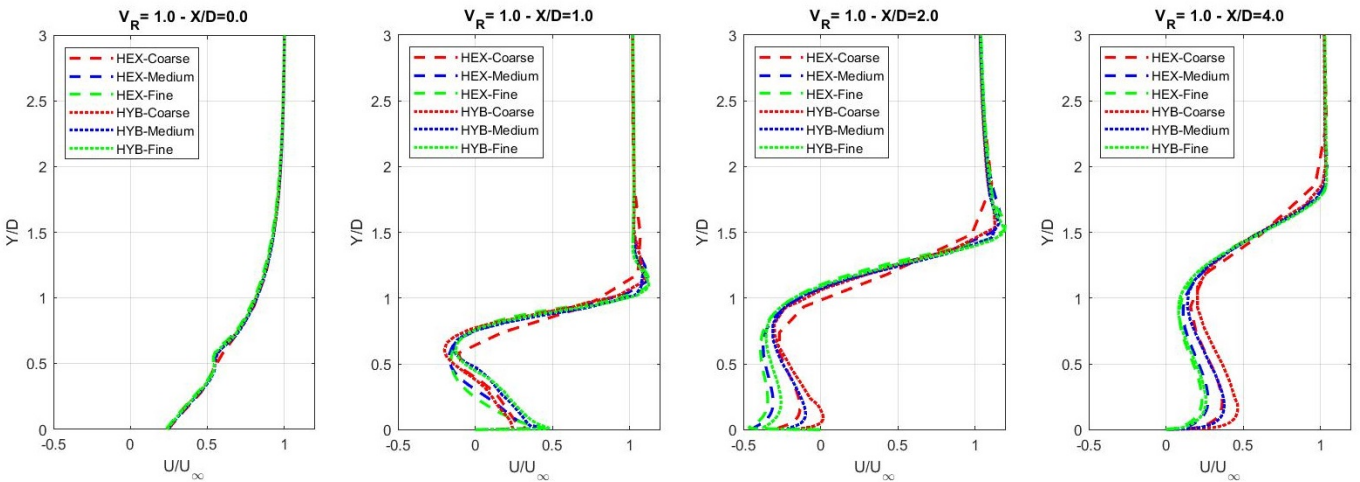


Figure 5. Grid Refinement effects on the numerical solution for $V_R = 1.0$

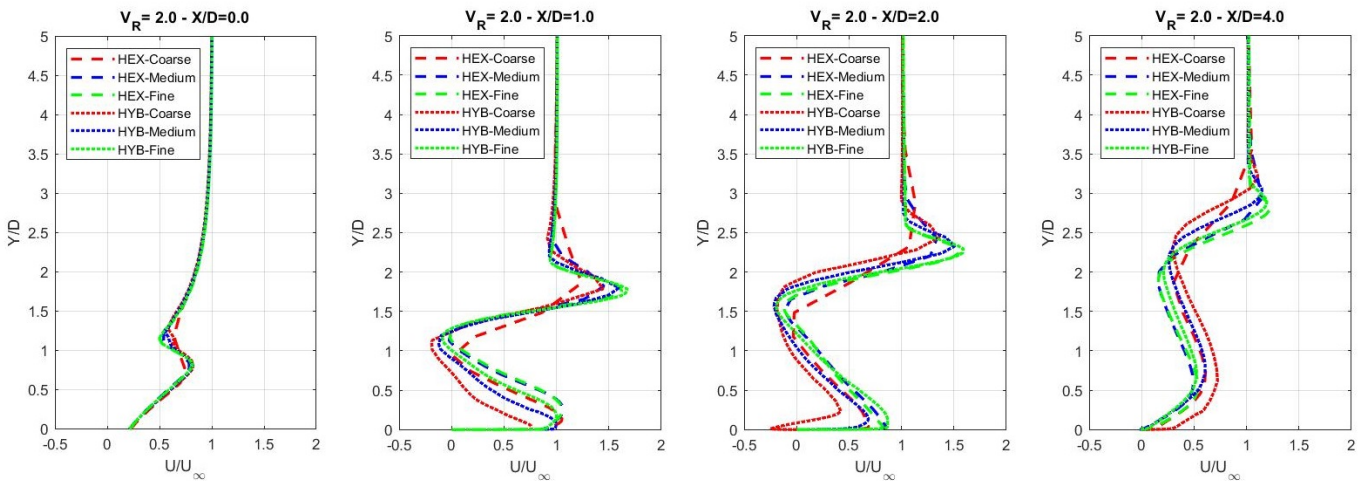


Figure 6. Grid Refinement effects on the numerical solution for $V_R = 2.0$

It was decided to perform the grid refinement study in several velocity ratios because this parameter can deeply change the flow behavior like the jet trajectory or the magnitude of the influence of the jet in the external flow. Thus, it is important to analyze the grid refinement effects for every velocity ratio to understand its effects on the numerical solution.

First, it is possible to verify that the effects of grid refinement on the numerical solution increases with the velocity ratio. Only small differences between the different meshes are observed for $V_R = 0.5$. However, as the velocity ratio increases, the distance between the curves becomes more pronounced in a way that one can clearly distinguish one curve to another at $V_R = 2.0$. This trend can be explained by differences in the jet path development as one change the velocity ratio. In higher velocity ratios, the jet path tends to lift away from the flat plate wall along the longitudinal positions, requiring every time more mesh refinement in vertical positions to properly solve the jet. As the coarser grids do not keep a high mesh resolution in further vertical positions, those meshes presents larger discretization errors as the velocity ratio increases. In the first longitudinal position at $X/D = 0$, the mesh refinement does not present meaningful differences for the whole range of velocity ratios analyzed, but in this longitudinal position the jet is starting its path along the flat plate and is located near the wall in region where all meshes present enough grid resolution.

The mesh refinement study for hexahedral and hybrid meshes showed a monotonic behavior, that is, at every refinement step the numerical results becomes closer to the finer grid. In addition, numerical results for the fine meshes presented in general a very good agreement to each other. However, it is important to remember that the hybrid fine mesh is around 35 per cent larger than the hexahedral one in terms of mesh size. It is interesting that the grid convergence behavior is different for booth mesh topologies, as the numerical results from medium hexahedral is much closer to the fine refinement level than the medium hybrid mesh. The same trend is seen for coarser grids. As an example, for $V_R = 1.0$ at $X/D = 2$, the result for medium hybrid is much closer to the coarse mesh, while the medium hexahedral mesh presented a result much closer to the fine mesh. Lastly, the medium hexahedral mesh presented results so close from fine hybrid and hexahedral meshes with about 8 times less expensive computationally than was the chosen mesh to proceed on the next analysis.

The velocity profiles predicted by Linear ($k-\varepsilon$ and *SST*) and Non-Linear (*Hellsten*) turbulence models are presented on the following figures for velocity ratios $V_R = 0.5, 1.0$ and 2.0 at the duct symmetry plane. Figure 7 presents the results in a plane positioned at the jet exit plane.

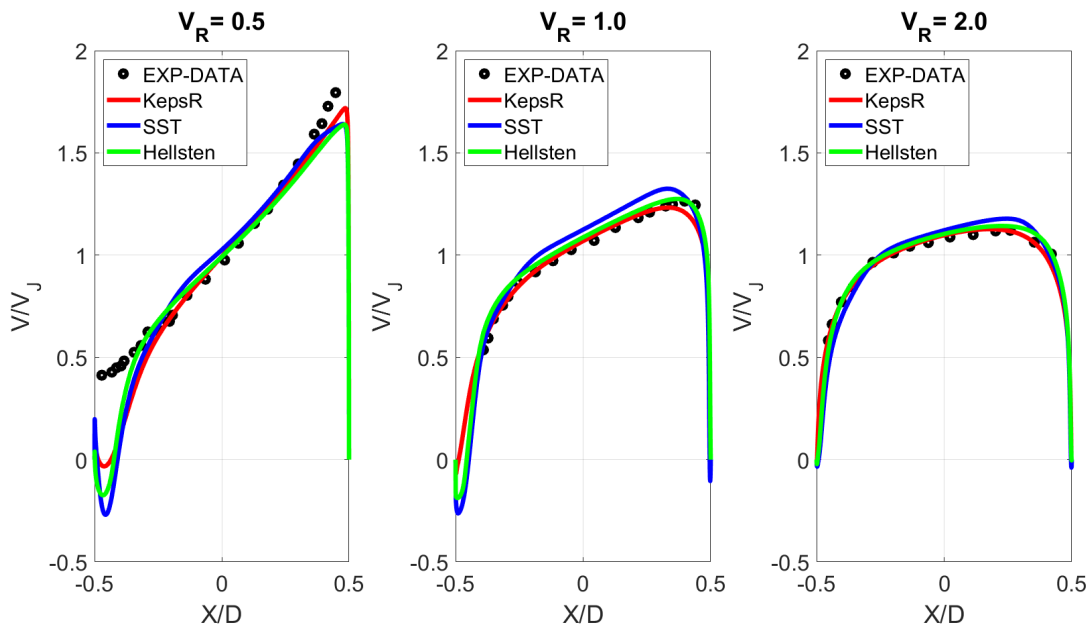


Figure 7. Velocity profile in the duct symmetry at the exit plane for different turbulence models

It is possible to see that as the velocity ratio decreases, the influence of the cross stream in the flow inside the duct becomes more intense and the velocity field also becomes more asymmetric, increasing the velocity at the exit hole trailing edge and reducing its magnitude at the hole leading edge. This trend is presented in the experimental work of Andreopoulos (1982) and is well captured numerically by all turbulence model tested in this work. At the exit plane, this effect is even more intense, and the numerical profiles shows a recirculation zone near the jet exit hole leading edge while the experimental data do not. It is interesting that the magnitude of the recirculation velocity is different and is pretty small for realizable $k-\varepsilon$ turbulence model. The *SST* model predicted a slight different velocity profile in the jet center line ($X/D = 0$) but is probably linked with a different development of the internal flow. Finally, no visible improvements with the *Hellsten* turbulence model was noticed, at least inside the duct.

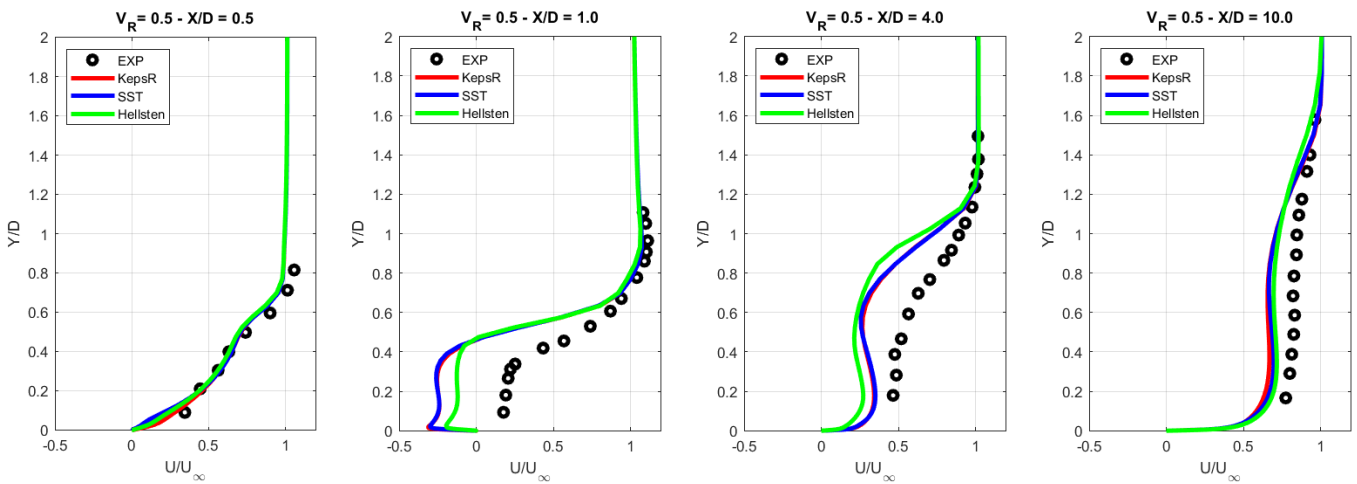


Figure 8. Velocity Profiles predicted by different turbulence models in the symmetry plane along the flat plate for $V_R = 0.5$

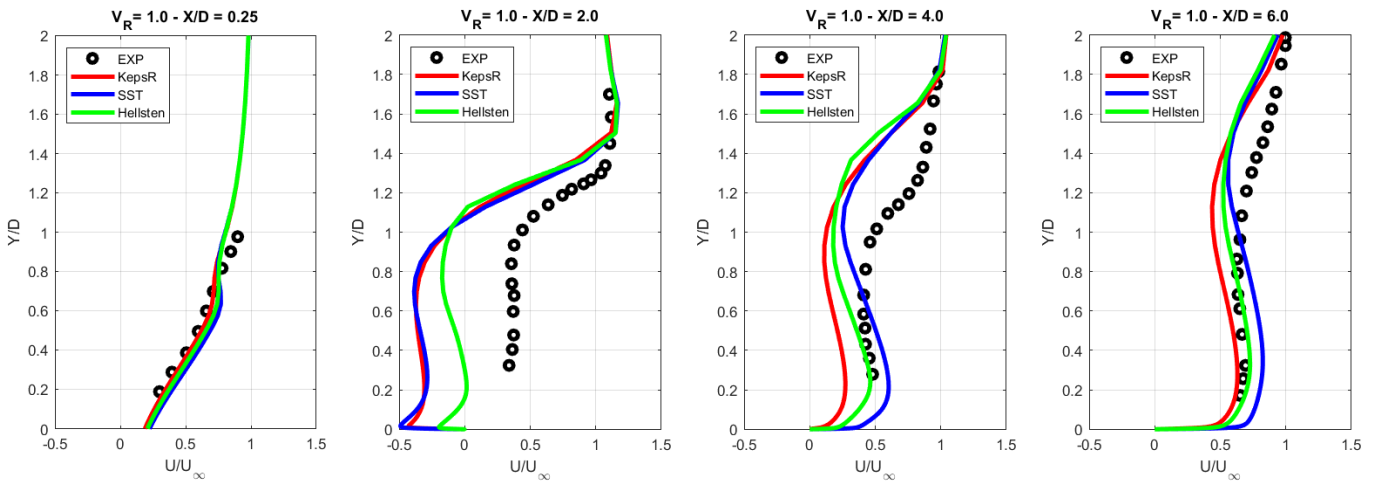


Figure 9. Velocity Profiles predicted by different turbulence models in the symmetry plane along the flat plate for $V_R = 1.0$

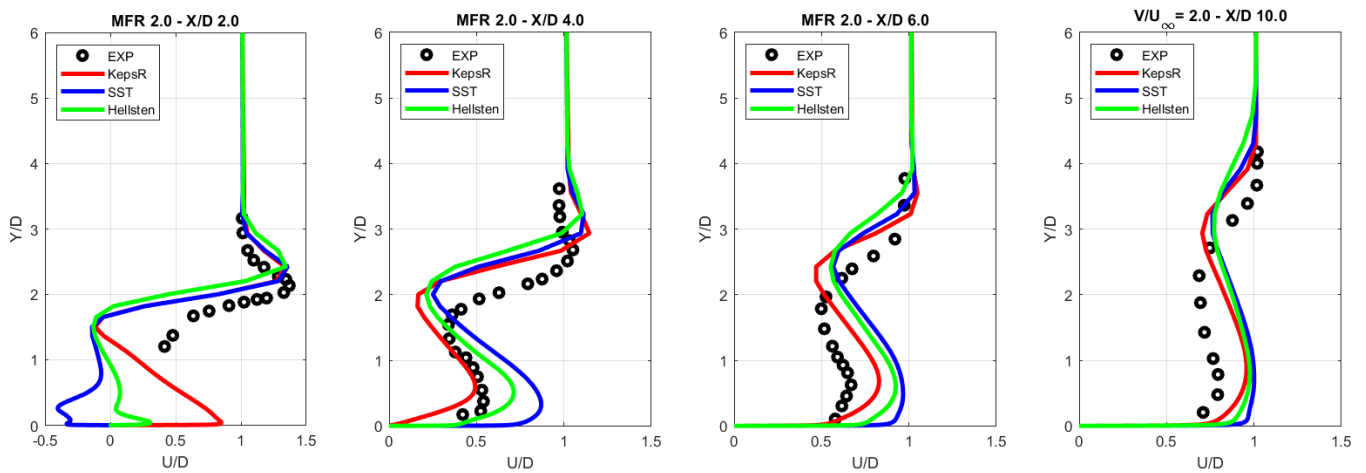


Figure 10. Velocity Profiles predicted by different turbulence models in the symmetry plane along the flat plate for $V_R = 2.0$

A comparison between experimental data from Andreopoulos and Rodi (1984) and numerical computations using different turbulence models mentioned in the previous sections are presented on figures 8, 9 and 10 for velocity ratios $V_R = 0.5, 1.0$ and 2.0 . Results are presented in terms of velocity profiles at the symmetry plane for several longitudinal positions.

In contrast with the relative good agreement between numerical and experimental data in the duct velocity profiles, the numerical flow field computations behind the jet lee presents a remarkable increase in error in comparison to the experimental data. First, it is important to mention that experimental measurements realized four diameters upstream the jet exit plane indicated a friction coefficient of $C_F = 0.0037$ and a boundary layer thickness of $\delta/D = 0.27$ while numerical computations showed $C_F = 0.0047$ and a boundary thickness of $\delta/D = 0.2$. Thus, the incoming boundary layer from numerical computations are slightly different from the experimental work. It is known that the flow field behind the jet lee can be affected by the boundary layer thickness (Andreopoulos, 1985) and this effect must be more studied afterwards. However, this effect is expected to be relatively small as the changes in boundary layer thickness are also small.

For the smaller velocity ratio, $V_R = 0.5$, the shape of the velocity profile is well captured by the numerical simulations, including the position where the jet effects become small and the position of the peak velocity. However, numerical simulations over predict the strength of the wake behind the jet. In section $X/D = 1.0$, for example, numerical profiles showed a recirculation zone while experimental data do not. Actually, this recirculation zone is expected for some velocity ratios, but most turbulence models over predict the extent of this zone. In this context, the *Hellsten* turbulence model show an improvement as it reduces the recirculation zone overpredicted by $k - \varepsilon$ and *SST*.

For $V_R = 1.0$ the velocity profiles predicted by the different turbulence models are very close for $X/D = 0.5$. At $X/D = 1.0$ a reversed flow zone appears for $k - \varepsilon$ and *SST* models up to $Y/D = 1$ which is in disagreement with experimental data. The *Hellsten* model reduces the strength of the reversed flow, but it still present in the numerical solution. At $X/D = 4.0$ and $X/D = 10.0$ there is no reversed flow anymore. The shape of the experimental velocity profile is approximately captured by numerical simulations, with a maximum error of the order $U/U_\infty = 0.5$.

For $V_R = 2.0$ the differences in the velocity profiles predicted by the turbulence models becomes more evident. Especially in the first analyzed section, $X/D = 2.0$, the profiles near the wall differ completely. The *SST* predicts a reversed flow near the wall, while the realizable $k - \varepsilon$ and *Hellsten* models shows positive or null velocity. Above the near wall region, the computed numerical results become much closer and the comparison against experimental data becomes better. Downstream the first position, the numerical computations near the wall over predicts the velocity near the wall, but the overall shape is capture with an error around $U/U_\infty = 0.3$ to experimental data.

Finally, the use of *Hellsten* turbulence model do not present the expected enhancement in predicting the velocity field for a jet in a crossflow. It is clear that it reduces some reversed flow regions, which do not appear in experimental data, but the overall profile still presenting a relatively high error in comparison with experimental data.

4. Conclusion and Final Remarks

In this work the effect of grid refinement and topology as well as the effect of different turbulence models have been studied for a jet in a cross flow with velocity ratios ranging from $V_R = 0.5$ to $V_R = 2.0$.

A different behavior in grid convergence was seen for hybrid and hexahedral meshes. Grid convergence was achieved sooner for hexahedral meshes, that is, for the same global refinement level, the computed velocity field for hexahedral meshes are more accurate. It is known that the jet position tends to move away from the flat plate wall as the velocity ratio increases requiring more grid refinement in upper vertical positions. As the meshes were created without adjusting the density zone with the velocity ratio because the jet trajectory is unknown in advance, the effects of global refinement become important for $V_R = 1.0$ and above. Coarse hybrid meshes, for example, could lead to a spatial discretization error up to $U/U_\infty = 0.5$ for $V_R = 2.0$ while the maximum error for $V_R = 0.5$ is around $U/U_\infty = 0.2$

The velocity profiles inside the duct presented a good agreement with experimental data for all velocity ratios. Only for $V_R = 0.5$, a slight difference was noticed as the numerical profiles predicted a small recirculation zone inside the duct which is not present in the experimental work. The velocity profiles computed with different turbulence models were very close to each other, the effect of turbulence modelling in this region is of second order inside the duct.

The development and entrainment of the jet in the cross stream was poorly predicted by every turbulence model tested. A slight improvement was observed for *Hellsten* model as it reduces the strength of reversed flow in regions where no reversed flow is expected according to experimental data. However, the overall comparison of the computed velocity field with experiment still poor.

In order to improve the accuracy of RANS models in computing jets in cross flow, it is important to understand the reasons that led them to failure, which is directly linked with the availability of experiments with detailed turbulence properties measurements. A lack of experimental data for jets in cross flow persists and future work must address this question.

5. ACKNOWLEDGEMENTS

I would like to express my very great appreciation to EMBRAER S.A. for sponsoring this work with computational resources for numerical simulations.

6. REFERENCES

- Andreopoulos, J., 1982. "Measurements in a jet-pipe flow issuing perpendicularly into a cross stream". *Journal Fluids Engineering*, Vol. 104, No. 4, pp. 493–499.
- Andreopoulos, J., 1985. "On the structure of jets in a crossflow". *Journal of Fluid Mechanics*, Vol. 157, pp. 163–197.
- Andreopoulos, J. and Rodi, W., 1984. "Experimental investigation of jets in a crossflow". *Journal of Fluid Mechanics*, Vol. 138, pp. 93–127.
- Bergeles, G., Gosman, A.D. and Launder, B.E., 1976. "The near-field character of a jet discharged normal to a main stream". *Journal of Heat Transfer*, Vol. 98, No. 3, pp. 373–378.
- Fric, T.F. and Roshko, A., 1991. "Structure in the near field of the transverse jet". *Turbulent Shear Flows*, Vol. 7, pp. 225–237.
- Hellsten, A.K., 2005. "New advanced $k - \omega$ turbulence model for high-lift aerodynamics". *AIAA journal*, Vol. 43, No. 9, pp. 1857–1869.
- Kamotani, Y. and Greber, I., 1972. "Experiments on a turbulent jet in a cross flow". *AIAA Journal*, Vol. 10, No. 11, pp. 1425–1429.
- Kelso, R.M., Lim, T.T. and Perry, A.E., 1996. "An experimental study of round jets in cross-flow". *Journal of Fluid Mechanics*, Vol. 306, pp. 111–144.
- Menter, F.R., 1994. "Two-equation eddy-viscosity turbulence models for engineering applications". *AIAA journal*, Vol. 32, No. 8, pp. 1598–1605.
- Morais, K.C., Abreu, D., Tobaldini, L., Papa, R. and Santos, L.C., 2018. "Effects of numerical modeling choices for heated jets in cross flow". International Council of the Aeronautical Sciences.
- Peroomian, O., Chakravarthy, S. and Goldberg, U., 1997. "A 'grid-transparent' methodology for cfd". In *35th Aerospace Sciences Meeting and Exhibit*. p. 724.
- Prause, J., Emmi, Y., Noll, B. and Aigner, M., 2016. "LES/RANS Modeling of Turbulent Mixing in a Jet in Crossflow at Low Velocity Ratios". In *54th AIAA Aerospace Sciences Meeting*. p. 0609.
- Ramsey, J.W. and Goldstein, R.J., 1971. "Interaction of a heated jet with a deflecting stream". *Journal of Heat Transfer*, Vol. 93, No. 4, pp. 365–372.
- Shih, T.H., Liou, W.W., Shabbir, A., Yang, Z. and Zhu, J., 1995. "A new $k - \varepsilon$ eddy viscosity model for high Reynolds number turbulent flows". *Computers & Fluids*, Vol. 24, No. 3, pp. 227–238.

7. RESPONSIBILITY NOTICE

The authors are the only responsables for the printed material included in this paper.